Int. J. Electrochem. Sci., 14 **(2019)** 7899 – 7910, doi: 10.20964/2019.08.49

International Journal of
ELECTROCHEMICAL
SCIENCE
www.electrochemsci.org

Activated Carbon Prepared from Rose Branch using H_3PO_4-hydrothermal Carbonization and Activation and its Apllication for Supercapacitors

Hongyu Si[1,2,*,#], *Bing Wang* [1,2,3,*,#], *Huiyuan Chen*[3], *Yonggang Li*[4], *Xiaodong Zhang*[5], *Xiaohui Liang* [1,2], *Laizhi Sun*[1,2], *Shuangxia Yang*[1,2], *Dong Hou*[6]

[1] Energy Institute, Qilu University of Technology (Shandong Academy of Sciences), Jinan, 250014, China
[2] Shandong Key Laboratory of Biomass Gasification Technology, Jinan, 250014, China
[3] College of chemical engineering, Qinghai University, Xining 810016, China
[4] School of Chemical Engineering, Baise University, Baise 533000, China
[5] College of Mechanical and Energy Engineering, Jimei University, Xiamen 361021, China
[6] Department of Materials Science and Engineering, Norwegian University of Science and Technology, 7491 Trondheim, Norway;
[*]E-mail: sihy@sderi.cn
[#]These authors contributed equally to this paper

Received: 23 March 2019 / *Accepted:* 20 May 2019 / *Published:* 30 June 2019

Charcoals of rose branch were prepared by the three different carbonization treatments: phosphoric acid hydrothermal method, traditional hydrothermal method and pyrolysis. Then these charcoals were activated under the same conditions to obtain activated carbons. It is found phosphoric acid plays two major roles: (1) improving the specific surface area and the pore volume of the charcoals; (2) increasing the reactivity of the charcoals, making charcoals easier to be activated. Electrodes using activated carbons from different carbonization methods were prepared, and electrochemical measurements were performed with a three-electrode cell using 1 M Na_2SO_4 as the electrolyte. Activated carbons prepared by conventional hydrothermal carbonization showed the lowest capacitance (137 F / g, at 0.2 A / g) and capacity retention (72.79%, at 2 A / g); while activated carbon prepared by phosphoric acid hydrothermal carbonization showed the highest specific capacitance (178 F / g, at 0.2 A / g) and capacity retention (91.01%, at 2 A / g).

Keywords: Activated carbons; Supercapacitors; H_3PO_4-hydrothermal carbonization; Rose branch; Capacitances

1. INTRODUCTION

Supercapacitors are electrochemical double-layered energy storage devices that can store electrical energy at the interface between the electrodes' charged surface and the electrolyte solution [1]. Activated carbon is widely used as electrode, and its porous structure can fit into the size of the electrolyte ions, forming an electric double layer capacitor (EDLC) [2]. The pore structure of activated carbons can be modified by the preparation process, which can provide a larger surface area for the migration of electrolyte ions, as well as increase the specific capacitance of the electrode [3].

Carbon-rich biomass feedstocks such as wood and straw can be used to prepare activated carbons [4,5]. Ornamental shrubs such as roses are widely planted around the world, and most of the shrub branches are directly discarded or incinerated during the pruning process, resulting in waste of resources and environmental pollution [6]. Rose branch (RB) is a high-quality raw material for the production of activated carbons because of its hard texture and high fixed carbon content [7]. At present, there are limited research on the RB based activated carbons.

Pyrolysis and hydrothermal are two most common carbonization methods to obtain charcoals. It requires heating raw materials to carbonization temperature in inert atmosphere and sealed water environment, and then hold for a period of time to obtain charcoals [8]. Hydrothermal carbonization is widely used in the preparation of charcoals for activated carbons due to its mild reaction conditions and low energy consumption [9]. However, the charcoals prepared by the traditional hydrothermal carbonization have a low specific surface area, a high concentration of functional groups, and a complicated chemical composition. Moreover, it is difficult to obtain activated carbons with well-developed pores structure after activation [10,11].

Phosphoric acid is a medium-strength protonic acid whose aqueous solution can promote the hydrolysis of cellulose and hemicellulose, and also can alter the structure of lignin [12]. In this study, a small amount of phosphoric acid was added in the hydrothermal carbonization stage to prepare charcoals with high degree of carbonization and strong reactivity, then the prepared charcoals were activated. The performances of charcoals prepared by conventional hydrothermal carbonization, phosphoric acid hydrothermal carbonization and pyrolysis carbonization, as well as the corresponding activated carbons after the same activation condition, were compared with each other by scanning electron microscopy, low temperature nitrogen adsorption apparatus, and electrochemical workstation.

2. EXPERIMENTAL PART

2.1. Preparation of activated carbons

RB (Pingyin, China) was cut into small pieces (length less than 1cm) and dried. 50 g of RB and 500 ml of different mass fractions (in a range of 0-9%) of phosphoric acid solution were mixed in a sealed reactor and carbonized at 180-270 °C for 2-8 h (the samples were referred as HC as followed). Another batch of RB was carbonized under N_2 flow (50 ml / min) at 400 °C for 2 h (referred as PC as followed).

Both HC and PC were mixed with a concentrated phosphoric acid solution to obtain slurries with a phosphoric acid/sample weight ratio of 3:1. The slurries were heated at 110 ° C for 2 h. Next, samples were activated under N_2 flow (50 ml / min) at 450 ℃ for 1 h at a heating rate of 5 ℃ / min. 0.1 M HCl was added to remove the ash in the samples, and the remaining solids were washed to neutral with deionized water. The activated carbon samples prepared from HC were designated as HAC; while the ones from PC was designated as PAC.

2.2. Characterization of activated carbons

The specific surface area and pore volume of the samples were measured by Brunauer-Emmett-Teller (BET) method and the average pore size was measured by Barrett-Joyner-Halenda (BJH) method using automatic specific surface area and average pore size analyzer (3h-2000ps4, Bei Shi De instrument).

2.3. Preparation of electrodes

Activated carbon samples were ground into powder, sieved through 300 meshes, then mixed with acetylene black and polyvinylidene fluoride (PVDF) with a mass ratio of 8:1:1. Then an appropriate amount of N-Methyl pyrrolidone was subsequently added to prepare a paste-like mixture. After magnetic stirring of the mixture for 4 h and ultrasonic treatment for 1 h, it was evenly coated on the cleaned aluminum foil, and then dried to semi-dry state at 60 ℃ before pressing. Finally, the tablets were dried at 110 ℃ for 12 h in vacuum and cut into activated carbon electrodes with a size of 1 cm^2.

2.4. Electrochemical measurements

The electrochemical performance test was carried out in the electrochemical workstation (PGSTAT 204, Switzerland Wan Tong) using the standard three-electrode system. The activated carbon electrodes were used as the working electrodes, platinum served as the counter electrodes, saturated calomel electrode was used as the reference, and 1 M Na_2SO_4 solution was used as electrolyte.

Constant current charge and discharge curves were measured at a current density between 0.2 and 2 A / g in a potential interval of 0–0.8 V. The specific capacitance from these measurements was obtained by Eq. (1)

$$C = \frac{I \times \Delta t}{m \times \Delta U} \quad (1)$$

where I, Δt, and ΔU represent the discharge current (A), the discharge time (s), and the potential interval (V).

2.5. Orthogonal Experiments

In order to systematically study the effects of different phosphoric acid hydrothermal carbonization factors on the specific surface area and pore volume of HC and HAC, an orthogonal test

chart L_{16} (4^3) as shown in Table 1 was designed. The factors include phosphoric acid mass fraction, temperature, and time during phosphoric acid hydrothermal carbonization. For each factor, four different levels were designed.

Table 1. Factors and levels of orthogonal experiments.

Factors / Levels	Carbonization temperature (°C) (A)	Carbonization time (h) (B)	Phosphoric acid mass fraction (%) (C)
1	180	2	0
2	210	4	3
3	240	6	6
4	270	8	9

3. RESULTS AND DISCUSSION

3.1. Results of Orthogonal Experiments

Table 2 shows the orthogonal test results of specific surface area and pore volume on HC and HAC samples. It is found the addition of phosphoric acid reduces the required temperature for carbonization of HC and HAC, while increases the specific surface area and pore volume of HC at low temperatures. The polysaccharides in the plant fiber are rich in hydroxyl groups [13], and the phosphoric acid can promote the dehydration of the polysaccharides and their hydrolysates, producing more gap structures. However, when the temperature reaches 270 °C, carbonization time and the presence of phosphoric acid have negligible effect on the specific surface area and pore volume of HC, indicating that most of the fiber raw materials are sufficiently hydrolyzed [14].

The effect of different factors and the levels of each factor on the specific surface area and pore volume of HAC and HC was compared by the orthogonal analysis, as shown in Table 3.There are two important parameters in the analysis: Ki is defined as the sum of the evaluation indicators at different levels (1, 2, 3, 4) in each of the influencing factors (A, B, C) [15]. Maximum Ki means the optimal level of each factor is obtained [16]. R stands for the extreme difference and is used to evaluate on what degree that different factors affect the outcome, i.e. a larger R value of a specific factor means it has a larger contribution of the outcome [17].For the specific surface area of HAC, the R values of the three factors were in an order of C>B>A; for the pore volume of HAC, the R values of the three factors were in an order of C>A>B. Therefore, the mass fraction of phosphoric acid (factor C) has the greatest influence on the specific surface area and pore volume of HAC. The addition of phosphoric acid in the hydrothermal carbonization improves the specific surface area and reactivity of the hydrothermal charcoals, making it easier to be activated to produce activated carbon with a well-developed pores and large specific surface area. On the contrary, the hydrothermal carbonization temperature and

carbonization time have little effect on the microstructures of activated carbons, similar observations had also been reported by Wu [18].

Table 2. Orthogonal experimental results of HC and HAC

	Factors of hydrothermal carbonization			HC		HAC	
NO.	Temperature(°C) (A)	Time(h) (B)	wt.% H_3PO_4 （C）	S_{BET} (m^2 / g)	V_{BJH} (ml / g)	S_{BET} (m^2 / g)	V_{BJH} (ml / g)
1	180	2	0	2.14	0.03	1084.85	0.98
2	180	4	3	7.42	0.07	1166.46	1.26
3	180	6	6	15.32	0.09	1673.37	1.31
4	180	8	9	17.15	0.12	1551.22	1.23
5	210	2	3	21.76	0.15	1407.31	1.11
6	210	4	0	10.43	0.06	1072.24	0.88
7	210	6	9	26.42	0.15	1792.16	1.28
8	210	8	6	23.15	0.16	1504.51	1.10
9	240	2	6	19.77	0.12	1630.66	1.12
10	240	4	9	25.32	0.16	1604.21	1.15
11	240	6	0	17.58	0.14	1065.87	0.76
12	240	8	3	20.61	0.17	1288.82	0.97
13	270	2	9	20.93	0.14	1477.43	1.05
14	270	4	6	22.01	0.14	1458.4	0.91
15	270	6	3	22.15	0.16	1463.59	1.04
16	270	8	0	22.20	0.15	986.01	0.71

Table 3. Analysis of orthogonal experimental results

Levels	Temperature(°C) (A)		Time(h) (B)		wt.% H_3PO_4 （C）	
	S_{BET} (m^2 / g)	V_{BJH} (ml / g)	S_{BET} (m^2 / g)	V_{BJH} (ml / g)	S_{BET} (m^2 / g)	V_{BJH} (ml / g)
K_1	1368.975	1.195	1498.748	1.0975	1052.243	0.8325
K_2	1444.055	1.0925	1325.328	1.05	1331.545	1.095
K_3	1397.39	1	1400.063	1.065	1566.735	1.11
K_4	1346.358	0.9275	1332.64	1.0025	1606.255	1.1775
R	97.697	0.2675	173.42	0.095	554.012	0.345

According to the Ki values of different levels, the optimum condition is $A_2B_1C_4$, meaning that the carbonization temperature is 210 °C, the carbonization time is 2 h, and the phosphoric acid mass fraction is 9%. At the optimum carbonization temperature and time, two kinds of hydrothermal charcoals were prepared by adding 9 wt.% H_3PO_4 (designated as HC-1) and H_2O (designated as HC-2), respectively. Then HC-1 and HC-2 were activated under the mentioned activation conditions to obtain

activated carbons and designated as HAC-1 and HAC-2 respectively. Table 4 describes the preparation conditions, specific surface area, and pore size of three kinds of charcoals (HC-1, HC-2 and PC) and three kinds of activated carbons (HAC-A, HAC-2 and PAC). Finally, the highest value activated carbon was observed from HAC-1, which has the highest specific surface area and the largest pore volume.

Table 4. Preparation conditions of charcoals and activated carbons from RB

Sample	Raw material	Mixed slurry	Temperature (°C)	Time （h）	S_{BET} (m^2 / g)	V_{BJH} (ml / g)
HC-1	RB	9 wt.% H_3PO_4	210	2	29.17	0.16
HC-2	RB	H_2O	210	2	9.36	0.05
PC	RB	-	400	2	2.86	0.005
HAC-1	HC-1	H_3PO_4: HC-1= 3	450	1	1803.26	1.33
HAC-2	HC-2	H_3PO_4: HC-2= 3	450	1	1079.21	0.86
PAC	PC	H_3PO_4: PC = 3	450	1	1221.78	0.64

3.2. Pore structure characterization

Fig. 1 depicts the N_2 adsorption isotherms and pore size distribution for charcoals and activated carbons. According to the IUPAC classification, the adsorption curves of charcoals, HC-1, HC-2 and PC, are close to type II, and the adsorption amount is small when the relative pressure is low [19]. With the increase of relative pressure (Fig. 1a), the adsorption amount of HC-1 and HC-2 was significantly higher than that of PC, indicating that hydrothermal carbonization is more conducive to pore formation than pyrolytic carbonization. HC-1 has a richer pore structure (Fig. 1c), indicating that the addition of phosphoric acid during the hydrothermal carbonization stage promotes the hydrolysis of the raw material fibers to produce a large number of microsphere gaps [20].

The adsorption curves of HAC-1, HAC-2 and PAC are close to the type I adsorption curve (Fig. 1b). When the relative pressure is low, the adsorption capacity increases rapidly, indicating that all three have abundant microporous structure [21], and the micropore volume were in the order HAC-1>PAC>HAC-2. With the gradual increase of pressure, the adsorption amount of PAC approaches the adsorption saturation state quickly, indicating that the pore structure of PAC is mainly microporous [22]. The adsorption amount of HAC-1 and HAC-2 was gradually increased, and a second rapid increase occurred after the relative pressure exceeded 0.9, indicating that HAC-1 and HAC-2 also have mesoporous and macroporous structures other than micropores [23]. The mesoporous and macroporous structure of HAC-1 is significantly more abundant than that of HAC-2, indicating that the addition of phosphoric acid during the carbonization phase contributes to the formation of mesopores and macroporous structures [24].

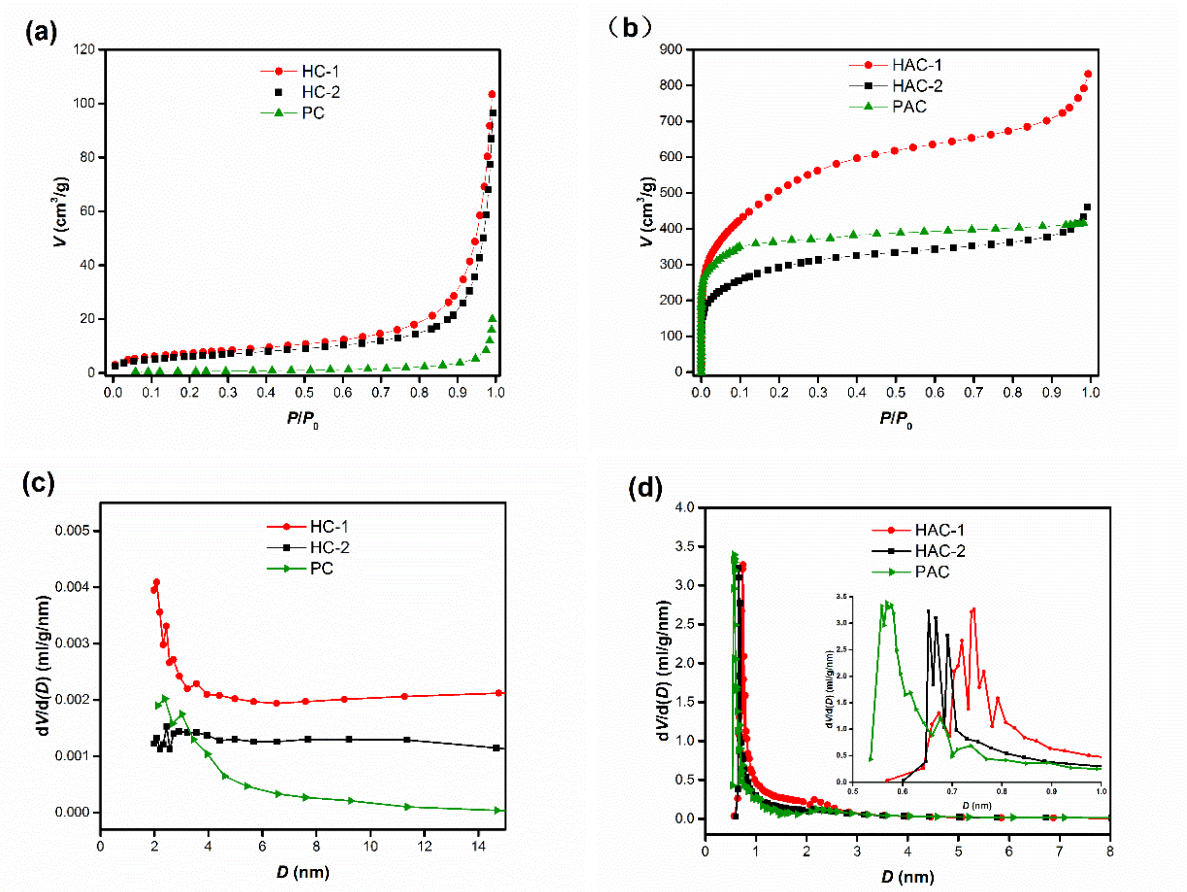

Figure 1. N_2 adsorption curves of charcoals and activated carbons (a, b) and Pore size distribution curves of charcoals and activated carbons (c, d)

According to the analysis of adsorption curve and pore distribution rule in Fig.1, the addition of phosphoric acid in hydrothermal carbonization stage improves the reactivity of charcoals, which can be more effective on the activators in the subsequent activation process. Sample HAC-1 has abundant microporous and mesoporous structures, and the most probable aperture is around 0.7-0.8 nm, which is beneficial to the diffusion of hydrated sodium ions (0.36 nm) and hydrated sulfate ions (0.38 nm), as well as the formation of electric double layer capacitors [25]. Therefore, the activated carbons prepared by phosphoric acid hydrothermal carbonization is a material which is very suitable for the electrodes.

3.3. Surface morphology analysis

Fig.2 shows the surface morphology of charcoals and activated carbons. The surface structure of HC-1 and HC-2 exhibit mesopores composed of microspheres, and phosphoric acid crosslinks microspheres into a more developed porous structure during the hydrothermal carbonization stage [26]. The surface structure of PC is smooth without obvious pore structure.

The surface of the sample HAC-1 forms a porous honeycomb structure, which provides a large number of effective areas and channels for the migration of electrolyte ions. Sample HAC-2 has irregular

surface morphology and less pore structure. The sample PAC exhibited a stacked sheet structure, indicating that the interior mainly contained a microporous structure with a smaller diameter [27].

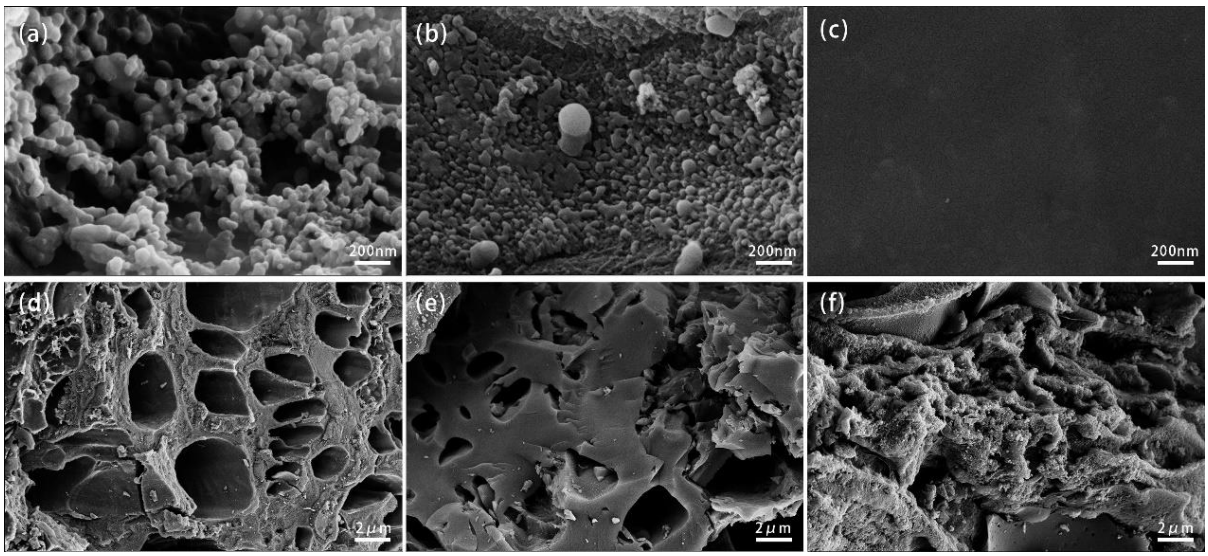

Figure 2. SEM images of HC-1(a), HC-2(b), PC(c) and HAC-1(d), HAC-2(e), PAC(f).

3.4. Electrochemical performance analysis

The samples HAC-1, HAC-2 and PAC were prepared into activated carbon electrodes and designated as HACE-1, HACE-2 and PACE, respectively. The electrochemical tests were carried out in 1M Na_2SO_4 solution. The cyclic voltammetry curves of three activated carbon electrodes (Fig. 3a) show no redox peaks, indicating that the surface of electrode mainly formed a double-layer capacitance with ion-absorbing and desorbing [28]. The curves of HACE-1 and HACE-2 are close to the typical rectangle of EDLC, which indicates the activated carbon electrodes prepared by hydrothermal carbonization have excellent double-layer capacitance characteristics [29]. The current of sample PACE increases slowly with the increase of potential, which is attributed to the higher content of micropore in activated carbon prepared by pyrolysis charcoal, and the higher resistance of micropores leads to the slower and more incomplete formation of electrochemical double layer [30]. Sample HACE-1 exhibits the largest response current due to large specific surface area and abundant mesoporous structure.

The constant current charge-discharge curves of the three activated carbon electrodes (Fig. 3b) show a symmetrical triangle shape, which indicates good electrochemical reversibility of the electrode materials [31]. The voltage drop of samples HACE-1 and HACE-2 was significantly lower than that of PACE during the process from charging to discharging, indicating that the activated carbons prepared by hydrothermal charcoals had lower equivalent series resistance and faster ion response [32]. Sample HACE-1 shows the longest charging and discharging time due to the higher specific surface area and the developed pore structure, which can provide more space for the storage of electrolyte ions, forming a fuller effective double layer behavior [33].

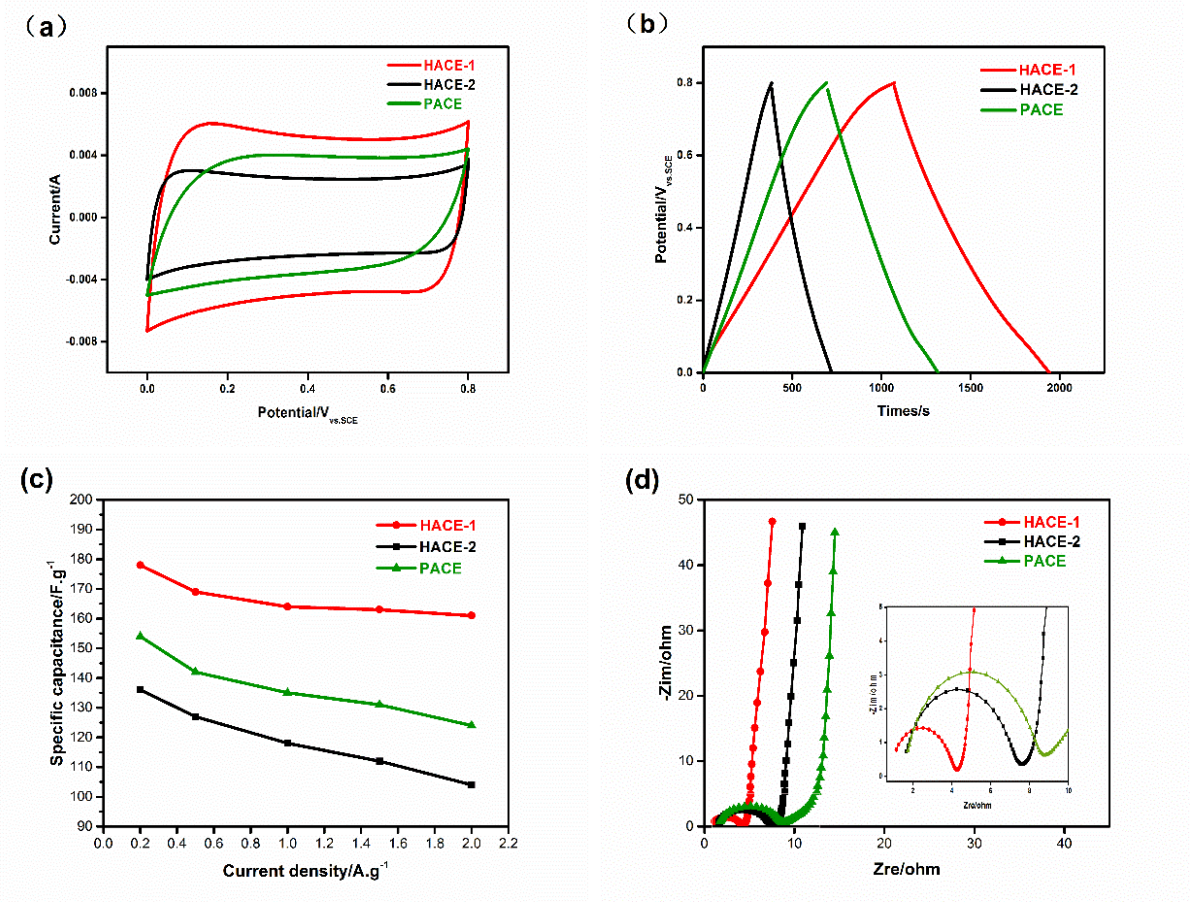

Figure 3. Cyclic voltammetry curves of activated carbon electrodes at 10 mV / s (a). Galvanostatic charge-discharge curves of activated carbon electrodes at 0.2 A / g (b). Specific capacitance of activated carbon electrodes at different current densities (c). Electrochemical impedance spectroscopy of activated carbon electrodes (d).

Table 5. The specific capacitance and capacitance retention of activated carbon electrodes at 0.2 A / g and 2 A / g.

Sample	*C* (F / g) (at 0.2 A / g)	*C* (F / g) (at 2 A / g)	Retention (%)
HACE-1	178	161	91.01
HACE-2	154	99	72.79
PACE	136	124	80.52

The specific capacitance of the three activated carbon electrodes are plotted against current density (Fig. 3c), and the specific capacitance decreases with increasing current density. Table 5 lists the specific capacitance and capacitance retention at 0.2 A / g and 2 A / g. Sample HACE-1 shows the highest specific capacitance of 178 F / g at 0.2 A / g, which is excellent for activated carbons. It also has the highest capacitance retention of 91.01% at 2 A / g. Samples HACE-2 and PACE show lower specific capacitance and capacitance retention due to low specific surface area and poor pore structure.

The impedance spectra of the three activated carbon electrodes (Fig. 3d) are depicted at the frequency range of 10 mHz-10 kHz and a disturbance amplitude of 5 mV for the sinusoidal wave. In the low frequency region, the three curves are close to the vertical line under ideal conditions, indicating that the capacitance characteristics are good [34]. The diameter of the semicircular arc of the curve in the high frequency region reflects the magnitude of ion migration resistance during charge and discharge of the electrode [35]. HACE-1 has the lowest ion mobility resistance due to its well-developed pore structure and good pore size distribution.

Table 6. Maximum capacitances of activated carbons from different precursors.

Biomass precursor	Activation method	S_{BET} (m^2/g)	Maximum capacitance	Capacitance measurement	Electrolyte	Reference
Coconut shells	H_3PO_4	1176	101	5mV/s	1M Na_2SO_4	[7]
Pistachio shell	KOH	1096	120	10mV/s	0.5 M H_2SO_4	[33]
Banana fibers	$ZnCl_2$	1097	74	0.5A/g	1M Na_2SO_4	[34]
Firwood	H_2O	1131	120	200mV/s	0.5 M H_2SO_4	[36]
cotton stalk	H_3PO_4	1481	114	0.5A/g	0.5 M Na_2SO_4	[37]
charcoal	H_2O	-	70	100mV	1M KCl	[38]
Rose branch	H_3PO_4	1803	178	0.2 A/g	1M Na_2SO_4	This work

The performances as supercapacitor electrodes of the activated carbons prepared from rose branch by H_3PO_4-hydrothermal carbonization and activation, was among the best reported for activated carbons prepared from a wide variety of biomass precursors (Table 6). Rose branch can therefore be successfully used to prepare porous activated carbons for EDLC applications. This is attributable to the development of a microporous network that is accessible to the electrolyte ions and is interconnected with small mesopores.

4. CONCLUSIONS

By comparing the properties of charcoals prepared by three carbonization methods, it was proved that the addition of phosphoric acid in the hydrothermal carbonization stage can promote the hydrolysis of fiber, improve the specific surface area and pore volume of charcoals. By comparing the performance of activated carbons obtained by three kinds of charcoals under the same activation conditions, the charcoal prepared by phosphoric acid hydrothermal carbonization has the highest reactivity. After carbonization and activation with phosphoric acid, RB show honeycomb structure connected by micropore and mesopore, which can provide a large number of effective areas and channels for

capacitance maintenance, reduce the migration resistance of electrolyte ions, and improve the stability and cycling performance of double-layer capacitors. Activated carbon with a specific surface area of 1803.26 m^2 / g, pore volume of 1.33 ml / g and the most probable pore size of 0.7-0.8 nm was obtained. The maximum capacitance obtained was 178 F / g at 0.2 A / g, and the capacitance retention rate was 91.01% at 2 A / g.

ACKNOWLEDGMENTS
This work was supported by the Special Fund for Agro-scientific Research in the Public Interest (201503135-04), National Key R&D Program of China(2018YFB1501403), the Natural Science Foundation of Shandong Province (ZR2016YL007), the "Chunhui Plan" of Ministry of Education PRC (Z2017039), the project of basic research for application from Qinghai Science &Technology Department (2017-ZJ-794).

References

1. I. Shown, A. Ganguly and L. Chen, *Energy. Sci. Eng.,* 3 (2015) 2.
2. S. Shafiei and R.A. Salim, *Energy. Policy.*, 66 (2014) 547.
3. O. Ellabban, H. Abu-Rub and F. Blaabjerg, *Renew. Sust. Energ. Rev.*, 39 (2014) 748.
4. J. Widen, N. Carpman and V. Castellucci, *Renew. Sust. Energ. Rev.*, 44 (2015) 356.
5. C. Gopal, M. Mohanraj and P. Chandramohan, *Renew. Sust. Energ. Rev.*, 25 (2013) 351.
6. G. Zhang, X. Lou and W.D, *Adv. Mater.*, 25 (2013) 976.
7. M. Zhang, Y.G. Li and B.Wang, *Int. J. Electrochem. Sci.*, 12 (2017) 7844.
8. X. Lu, M. Yu and T. Zhai, *Nano. Lett.*, 13 (2013) 2628.
9. J. Hou, C. Cao and F. Idrees, *ACS. Nano.*, 9 (2015)2556.
10. G. Yu, S. Yano and H. Inoue, *Appl. Biochem. Biotechnol.*, 160 (2010) 539.
11. W. Zhang, H. Tao and B. Zhang, *Carbon*, 49 (2011) 1811.
12. M. Mastragostino, C. Arbizzani and F. Soavi, *Solid. State. Ionics.*, 48 (2002) 493.
13. N.H.N. Azman, Y. Sulaiman, M.S.M. Nazir and H.N. Lim, *J. Mater. Sci-Mater. El.*, 14 (2019) 58.
14. R. Kotz and M. Carlen, *Electrochem. Acta.*, 45 (2000) 2483.
15. C. W. Liew, S. Ramesh and A.K. Arof, *Mater. Design.*, 92 (2016) 829.
16. C. W. Liew, S. Ramesh and A.K. Arof, *Energy*, 109 (2016) 546.
17. E. Frackowiak, Q. Abbas and F. Béguin, *J. Energy. Chem.,* 22 (2013) 226.
18. Z. Liu, A. Quek, S. Kent Hoekman and R. Balasubramanian, *Fuel,* 103 (2013) 943.
19. A. C. Lua and J. Guo, *Carbon*, 38 (2000) 1089.
20. A. Elmouwahidi, Z.Z. Benabithe and F.C. Marín, *Bioresource. Technol.*, 111 (2012) 185.
21. A. Ahmadpour and D.D. Do, *Carbon*, 35 (1997) 1723.
22. C. Saka, *J. Anal. Appl. Pyrol.*, 95 (2012) 21.
23. S. Mitani, S. I. Lee and K. Saito, *Carbon*, 43 (2005) 2960.
24. C. Zhou, Y. Zhang and Y. Li, *Nano. Lett.*, 13 (2013) 2078.
25. Y.E. Miao, W. Fan and D, Chen, *ACS. Appl. Mater. Inter.*, 5 (2013) 4423.
26. J. Han, G. Xu and B. Ding, *J. Mater. Chem.* A., 2 (2014) 5352.
27. M.A.B. Fathallah, A. B. Othman and M Besbes, *Appl. Phys. A-Mater.*, 124 (2018) 120.
28. Y. Sun, G. Yang and J. Zhang, *Chem. Eng. Technol.*, 35 (2012) 309.
29. D, Prahas, Y. Kartika and N. Indraswati, *Chem. Eng. J.,* 140 (2008)32.
30. V.O. Njoku, M.A. Islam and M. Asif, *J. Environ. Manage.*, 154 (2015)138.
31. B.S. Girgis, A.A. Attia, N.A. Fathy, *Colloid. Surface.* A., 299 (2007) 79.
32. M. Zhi, A. Manivannan and F. Meng, *J. Power. Sources.*, 208 (2012) 345.

33. F.C. Wu, R.L. Tseng and C.C. Hu, *J. Power. Sources.*, 144 (2005) 302.
34. V. Subramanian, C. Luo and A.M. Stephan, *J. Phys. Chem.* C., 111 (2007) 7527.
35. R. Sharma and S. Suhag, *J. Mar. Eng. Technol*., 1 (2018) 11.
36. F.C. Wu, R. L. Tseng and C.C. Hu, *J. Power. Sources.*, 138 (2004) 351.
37. M. Chen, X. Kang, T. Wumaier, J. Dou and B. Gao, *J. Solid. State. Electr.*, 17 (2013) 1005.
38. P. Shabeeba, M.S. Thayyil, M.P. Pillai and Soufeena, *Russ. J. Electrochem.*, 54 (2018) 302.